LAWRENCE
LIVERMORE
NATIONAL
LABORATORY

LLNL-TR-457951

UEDGE Simulations of CMOD Discharge 1100212014

G. D. Porter

September 30, 2010

This work performed under the auspices of the U.S. Department of Energy by Lawrence Livermore National Laboratory under Contract DE-AC52-07NA27344.

Memo

To: DIII-D 2010 Joule Milestone Team

From: G D Porter

CC: Brian LaBombard

Date: 24 September 2010

Re: UEDGE simulation of CMOD discharge 1100212024.01360

1 Introduction

We report here initial UEDGE[1] simulations of CMOD discharge 1100212024. This discharge was taken as part of Joint Research Task (JRT), i.e. a coordinated effort between several diverted tokamaks to characterize the heating flux on the divertors when the devices were operated in similar geometries. The tokamaks included in this exercise were CMOD, DIII-D and NSTX. Discharges taken as part of this coordinated effort on DIII-D are also being analyzed using UEDGE and will be reported elsewhere.

This report begins with a brief description of the CMOD discharge in Section 2, followed by a detailed description of the simulation results with a variety of different physics assumptions in Section 3.

2 Discharge Description

CMOD discharge 110212024 was taken 12 February, 2010 as part of a campaign to obtain data with dimensionless similar discharges with DIII-D and NSTX. This CMOD discharge was described in some detail at the 2010 PSI conference in San Diego.[2] The discharge is an "Enhanced D_α" (EDA) high confinement (H-mode) discharge. The magnetic reconstruction obtained using EFIT[3] indicates this discharge is a Lower Single Null (LSN) with a fairly narrow gap, i.e. the limiter surfaces maps to only 8.1 mm from the separatrix at the Low Field Side (LFS) midplane. The UEDGE mesh obtained using this EFIT reconstruction will be shown in the next section. The plasma is heated with a combination of Ohmic (0.63 MW) and ICRH (3.86 MW). There is 1.92 MW of radiated power on the closed field lines yielding an estimated power into the Scrape-off layer (SOL) of 2.17 MW (0.9*PICRF minus Prad_core). Diagnostics that are available to guide the UEDGE simulations include an edge Thomson Scattering (TS) system measuring the electron density and temperature near the separatrix, an array of Langmuir probes in the divertor region that nominally determine the plasma density, ion saturation current, plasma potential and electron temperature at the divertor floor; and an Infra-red TV system (IRTV) measuring the heat flux profile on the outer divertor. These data are provided by Brian LaBombard with the proviso that data not be distributed without permission of the C-mod experiment. We will show comparisons of the experimental data and UEDGE simulations in this report.

3 UEDGE simulations

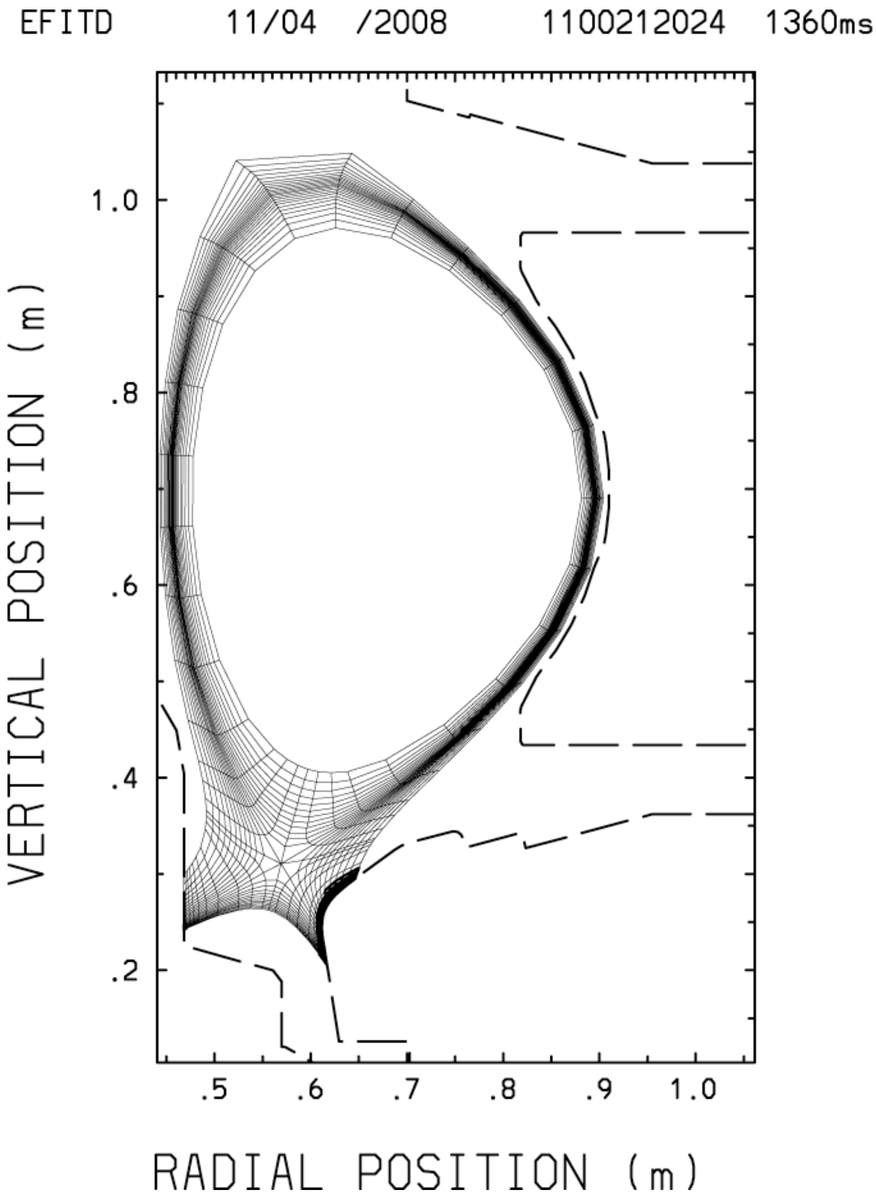

Figure 3-1 UEDGE mesh used for simulation of CMOD discharge 1100212024.

The UEDGE mesh obtained using the data from the EFIT reconstruction of CMOD discharge 1100212024 is shown in Figure 3-1. The radial region used for the simulations extends inside the last closed flux surface (LCFS) to the 90% poloidal flux (Ψ_N=0.90) and out to the limiting surface at Ψ_N=1.05. We use a non-orthogonal mesh that closely matches the divertor geometry of the machine. The mesh contains 49 poloidal cells, concentrated near the divertor plates where we expect plasma parameters to vary most quickly, and 23 radial cells, concentrated near the separatrix.

The UEDGE code requires a variety of options for physics to be included and the use of boundary conditions at all surfaces that define the calculation domain. These include:

- We use the mesh described previously and shown in Figure 3-1 for all simulations discussed in this memo.
- We solve plasma fluid equations for the ion density, the ion and electron thermal transport, the ion parallel momentum and the plasma potential. A simple model for potential, which solves Ohm's law on the open surfaces of the SOL, but which is probably not accurate on the closed surfaces in used in Section 3.1. A more accurate potential model is incorporated when

we include the effect of plasma drifts[4] in Section 3.2. All equations are iterated to obtain a steady state solution with residuals less than 10^{-8}.

- The radial power across the inner-most flux surface, Ψ_N=0.90, is specified as a boundary condition (BC). We assume the experimentally determined power is distributed equally between power flowing in the electron channel and that flowing in the ion channel, i.e. 1.1 MW in each.

- The ion density on the inner-most flux surface is specified as a BC and is assumed constant on that surface. We use the value measured with the TS diagnostic to specify this density.

- We specify the BC on the ion density at the outermost and private flux (PF) surfaces by assuming the radial scale length of the density falls off with a 10 cm scale length. The ion flux resulting from this assumption is recycled as neutral deuterium atoms.

- We use a fluid model for simulating the neutral density. This model includes the effect of momentum exchange with the deuterium ions and inertial effects, i.e. we include simulation of the parallel neutral momentum.[5] The ion flux flowing to the outer-most and PF surfaces as well as that flowing to the divertor plates is assumed to recycle as neutral atoms. The BC used for the neutral density at these surfaces is specified as a neutral albedo at each surface. The assumed albedo at both the inner and outer plate is assumed to be 0.99 (1% of the neutral flux to these surfaces is removed or pumped); that at the outermost flux surface is assumed to be 0.95 and that at the PF surface is assumed to be 1.0.

- We assume all anomalous transport is diffusive. Initial simulations, discussed in Section 3.1.1, assume that the electron and ion thermal diffusivity and the particle diffusivity are spatially constant. Subsequent simulations assume a radially varying particle diffusivity. The value of all diffusivities is varied to obtain better agreement with experimental data.

- The BC used for the neutral density at the boundary of the calculation means that all surfaces are pumped. Initially the only ion source that is required to obtain steady state is an ion flux across the innermost flux surface. We note that the neutral density at the LFS midplane is quite high so we introduce a gas puff at that point. The amplitude of this gas puff is assumed to be 100 atom A. We discuss the effect of this gas puff in Section 3.1.3, and use it in Section 3.2.

-

3.1 Simulations without drift effects

3.1.1 Initial simulations, spatially constant particle and thermal diffusivity

The upstream and divertor profiles obtained in the initial UEDGE simulation, BLc02, (run BLc01 mistakenly used an old geometry for the inner divertor plate) are compared with experiment in Figure 3-2. This simulation was done with spatially constant thermal, particle and momentum diffusivities of:

$$\chi_i = \chi_e = 0.1 m^2/s$$
$$D = 0.1 m^2/s$$

Equation 1

All parameters are mapped to the LFS midplane and plotted versus the distance from the separatrix at that poloidal position. Although there are discrepancies between experiment and simulation on all the profiles, the density profile is most poorly fit with the assumptions used for this simulation. Based on experience in simulating DIII-D discharges we chose to introduce a radially dependent particle diffusivity to improve the density profile.

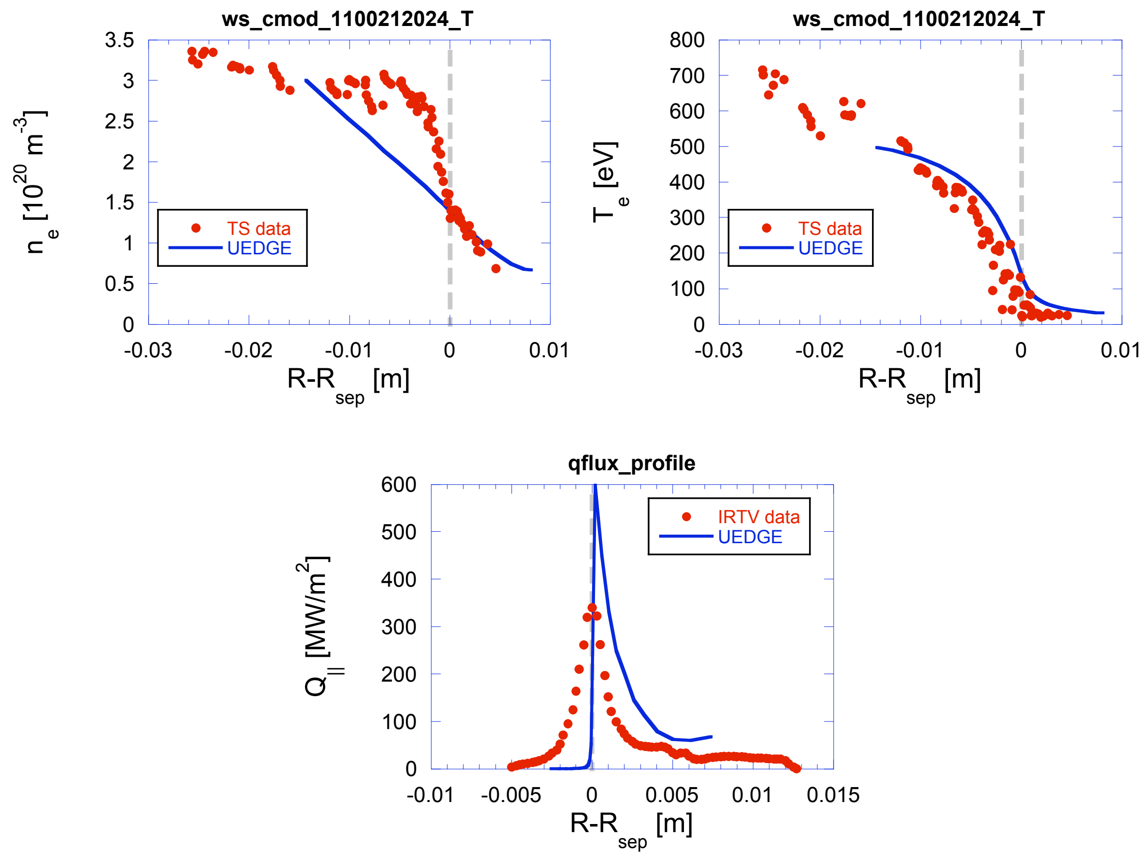

Figure 3-2 Comparison of measured upstream plasma profile and divertor heating profile with UEDGE simulation BLc02. Only the heating profile at the outer divertor is shown, corresponding to the experimental measurement.

3.1.2 Effect of radially dependent particle diffusivity

The problem was divided into three radial zones to modify the particle diffusivity. Zone 1 is from the innermost flux surface to the surface that lies 0.4 cm inside the separatrix at the LFS midplane. Zone 2 goes from 0.4 cm inside to 0.3 cm outside the separatrix and zone 3 extends from there to the edge of the calculation domain, 8 cm outside the separatrix. We show two simulations in Figure 3-3 to demonstrate that although the density profile can be made more consistent with experiment by simply introducing the particle transport barrier in zone 2, we had to modify the thermal diffusivity to bring the electron temperature back to the experiment after reducing the diffusivity in zone 2. The first simulation, BLc05, used the particle diffusivity in zone 2 of 0.015 m^2/s, leaving all other diffusivities the same as in Equation 1. This simulation has a significantly higher electron temperature on the core surface than the experiment. We had to increase the thermal and momentum diffusitivities to 0.16 m^2/s to make the electron temperature more consistent with experiment (run BLc05b). It is interesting to note that simulation of DIII-D plasmas typically do not require iteration of the thermal diffusivity after introducing a radially dependent particle diffusivity. The radial power flow is composed of a convective part, associated with the power carried by the radial particle flux, and a conductive flow associated with the radial transport due to anomalous diffusion, as shown in Equation 2. One can solve the simplified form of this equation for the temperature on the core surface for a specified power (recall that the power is used as a BC in UEDGE) showing that the core temperature is determined by the sum of the inverse scale length of the temperature and density on that surface. In DIII-D the convective term, D/λ_n, is small. The density scale length increases for both CMOD and DIII-D when one introduces a particle transport barrier at the separatrix (the density flattens), but since the convective term is small in DIII-D, the electron temperature on the core typically does not change. However, the convective and conductive contributions to the radial power are more equal for CMOD so that one has to modify the thermal diffusivity when the core density flattens out.

$$P_r \propto -\chi n \frac{\partial T_e}{\partial r} - 2.5TD\frac{\partial n}{\partial r}$$
$$\propto -nT\left(\frac{\chi}{\lambda_T} + \frac{D}{\lambda_n}\right)$$

Equation 2

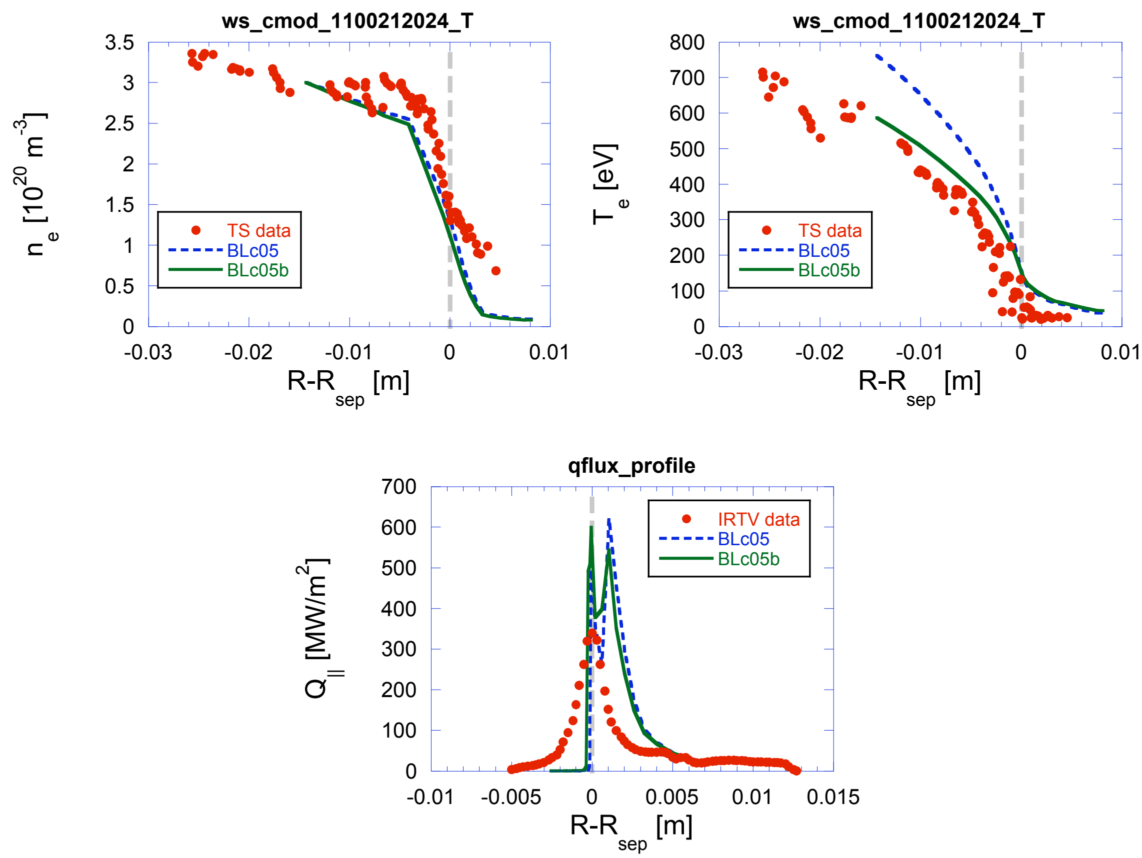

Figure 3-3 Comparison of measured upstream plasma profiles and divertor heating profiles with UEDGE simulations with radially dependent particle diffusivity.

The simulated density profile on the closed field lines is more consistent with experiment when a particle transport barrier is introduced near the separatrix. However, the SOL density is much lower than experiment. Upon examining the data Brian LaBombard sent us we noticed that the neutral density near the LFS midplane was quite high. We therefore introduced a neutral gas puff in a region near the midplane, extending about 20 cm poloidally. The effect of this gas puff is discussed in the next section

3.1.3 Effect of gas puff at LFS midplane

The effect of a 100 atom Amp (about 1000 Torr l/s) gas puff is shown in Figure 3-4. There is remarkably little effect on the upstream plasma profiles. The effect of the gas puff on the ion saturation plate is also shown in this figure. The UEDGE sign convention is that a current flowing clockwise (from the inner plate toward the outer plate) is positive. Hence ion current flowing to the inner plate appears negative and that to the outer plate is positive. The divertor heat flux in a very narrow region near the strike point increases more than a factor of 2 with the gas, arising from the sharp spike in J_{sat}. The ion flux across the core surface is about 270 atom Amp so the 100 A introduced by the gas puff is only a perturbation which increases the recycling currents a bit. There is very little effect on the SOL density. All subsequent simulation results described in this memo include this gas puff.

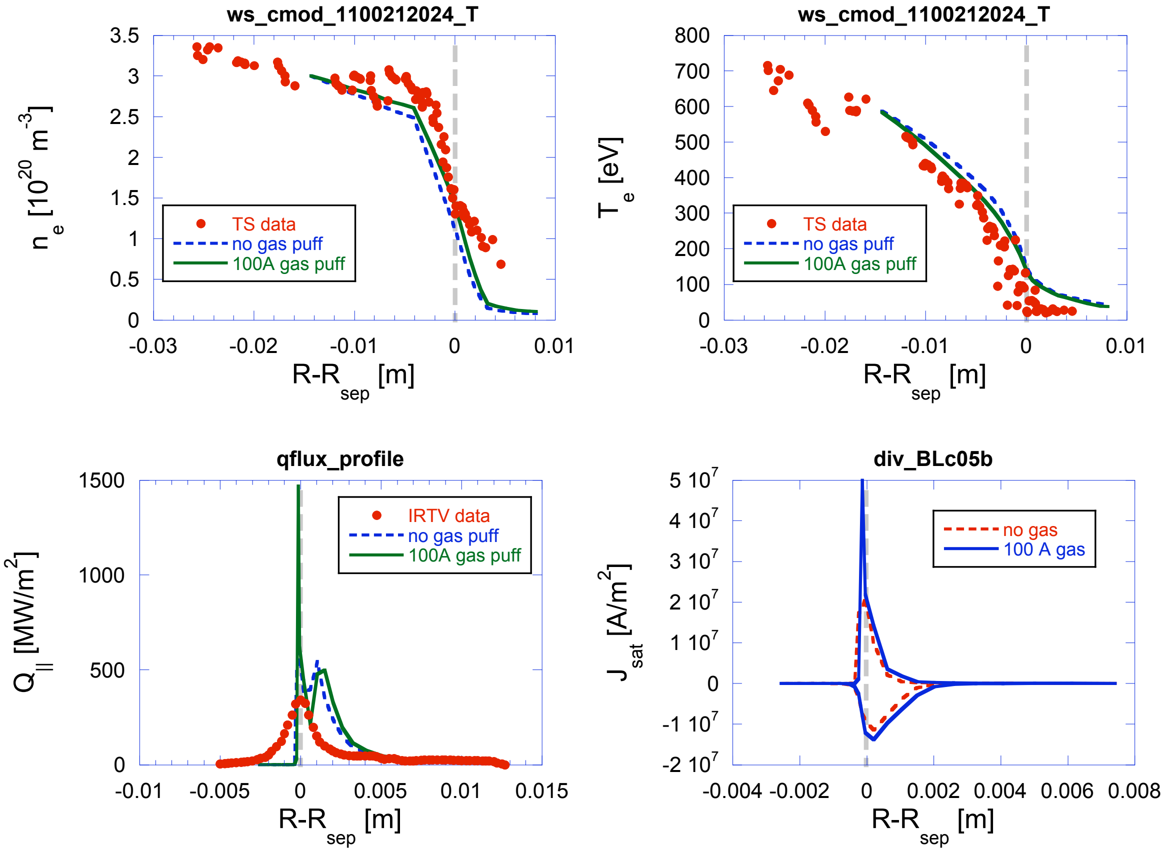

Figure 3-4 Comparison of upstream plasma profile and divertor heating profile with UEDGE simulations with and without a 100A gas puff at the LFS midplane.

3.2 Simulations with drift effects

The final set of physics that we have implemented for these simulations of CMOD has been the inclusion of the effect of all plasma drifts, ExB, ∇B and ∇P.[4] It has been proposed that the effect of these drifts is important for DIII-D.[6] We find that they are even more important for CMOD. The cross field diffusivities had to be modified to keep the upstream plasma profiles more or less consistent with experiment. The upstream and divertor profiles are compared with experiment in Figure 3-5. The diffusivities used for this simulation are:

$$\chi_i = \chi_e = 0.05 m^2 / s$$
$$D_1 = D_3 = 0.05 m^2 / s$$
$$D_2 = 0.075 m^2 s$$

Equation 3

Note that the scale used for the ordinate of the divertor parameters in Figure 3-5 has been expanded to better see the profiles obtained with drifts. The high divertor heating flux near the strike point is therefore not obvious, nor is the peak in the ion saturation current. The level of these features without drifts can be seen in Figure 3-4. The amplitude and shape of the divertor heating flux and ion saturation current are more consistent with measurement for the simulation that includes the effect of drifts. The experimental ion saturation current appears to peak in the PF region that seems unlikely and may indicate some uncertainty in the location of the strike point. Unfortunately the probe data on the inner plate has a wide gap where UEDGE shows the largest flux to the plate.

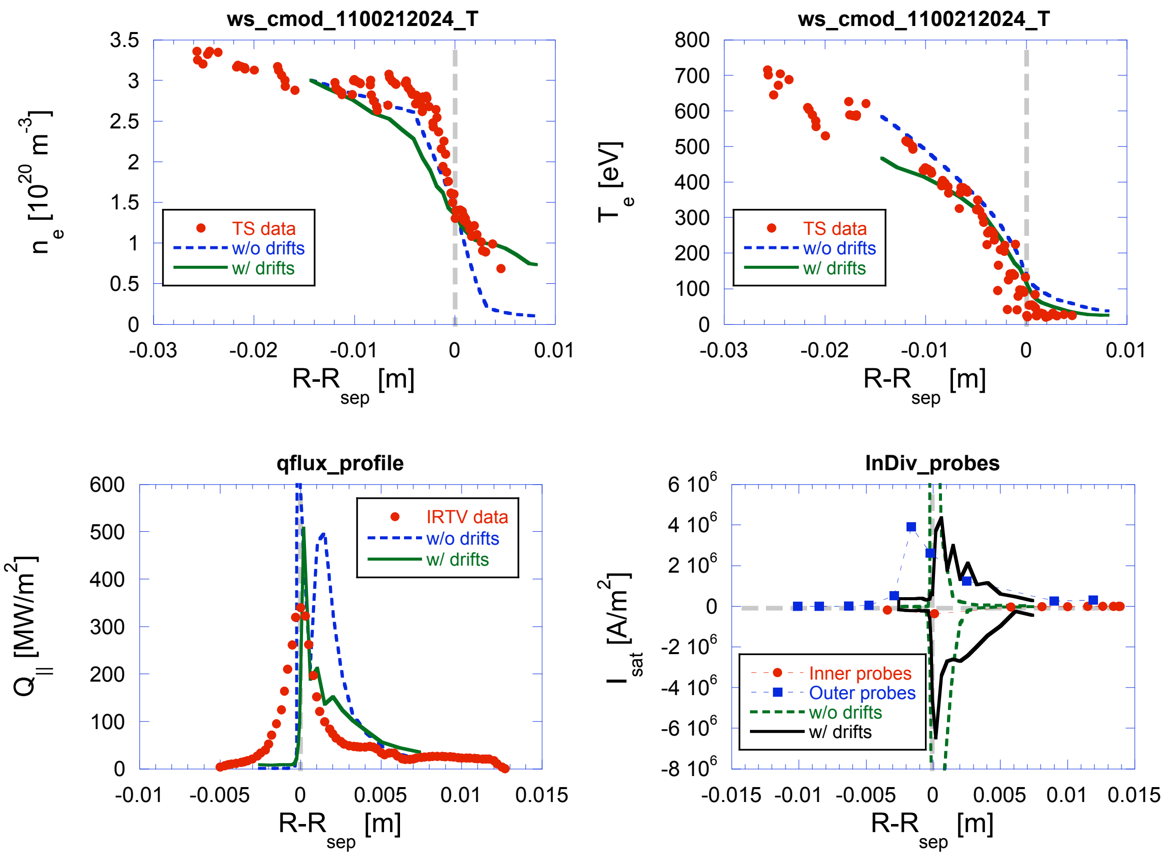

Figure 3-5 Comparison of upstream and divertor parameters with UEDGE simulations without drifts (BLc07) and with drifts (BLc13).

$$nT \propto \beta B^2$$
$$v_{drift} \propto 1/B$$
$$\Gamma_{drift} = nv_{drift} \propto \frac{\beta B}{T}$$

Equation 4

One possible view of the importance of the effect of drifts is seen by examining the scaling of the drift flux with the total field B, as shown in Equation 4. Plasma drift velocities scale as 1/B, suggesting that the drifts are less important for high field devices such as CMOD. However, if one chooses to maximize the use of the expensive magnetic field, i.e. operate near a MHD limited plasma pressure, the drift fluxes will scale as B and therefore are more important for high field devices such as CMOD (and ITER). One should compare these drift fluxes with those expected from anomalous diffusion. However, that would bring in the unknown particle diffusivity. The size scaling of particle diffusivity is not known. Furthermore there is fear that the diffusive fluxes obtained in these simulations are dominated by numerical diffusion associated with the use of “upwind differencing”. This concern is particulary worrisome for a case with the extremely small diffusivities needed to match the upstream profiles for the CMOD simulation with drifts (see Equation 3) The numeric diffusion problem is currently understudy by not only UEDGE developers, but by developers of other fluid edge plasma codes.

Finally, we show the effect of drifts on the 2D profile of D_α emission in Figure 3-6. We show these profiles in the hope there might be some experimental data which can be compared with the simulations and therefore confirm the importance of including drifts in simulations of the edge plasmas.

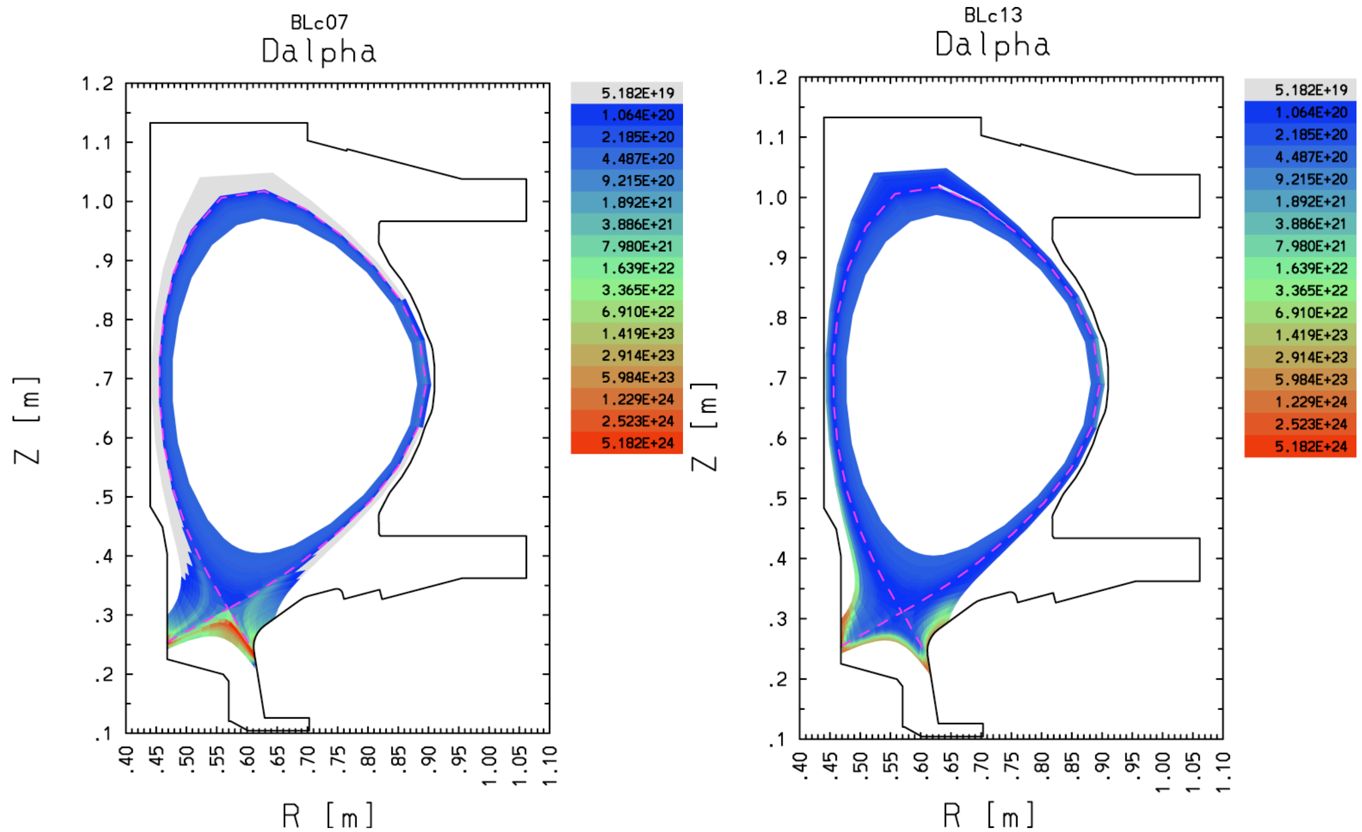

Figure 3-6 Comparison of D_α emissivity for a simulation without drifts (left, BLc07) and one with drifts (right, BLc13).

4 Summary and conclusions

We report initial results of UEDGE simulations of a CMOD discharge taken as part of coordinated research effort to characterize the divertor heating characteristics on several devices. We have discussed the sensitivity of the simulation results to numerous UEDGE input parameters and physics models. We find that the code is able to reproduce the experimentally measured divertor heating profile when all relevant physics are turned on, viz. when the effect of plasma drifts is included. Reproduction of the measured upstream plasma profiles on CMOD requires use of a radially dependent transport model for particle diffusivity. We find that the high density of CMOD discharges requires iteration of the thermal transport diffusivity when the particle transport model is modified. This is not characteristic of simulations of DIII-D data and indicates that convective power flow in CMOD is a larger fraction of the total cross-field power flow in CMOD. Furthermore we find that inclusion of plasma drifts in CMOD has a dramatic difference in the nature of the divertor plasmas. We show that one expects drifts to be more important for a high field device when operated near a plasma β limit. Thus the higher density of a high field device makes the inclusion of plasma drifts essential. This should be a concern for simulations of the ITER device.

CMOD simulations with plasma drifts require use of very small cross-field diffusivities since much of the radial plasma flow arises from the effect of drifts. The use of small diffusivities is problematic for UEDGE since numeric diffusion associated with the differencing scheme becomes larger than that determined from the assumed transport model. The resulting numerical problem has led to CMOD simulations which have spatial oscillations which we do not believe are real. This numeric diffusion has been a recognized problem in all fluid edge plasma codes. Recently a re-formulation of the numerical scheme used for these simulations has been proposed as a solution to this problem. This scheme has been implement in UEDGE. We have not yet applied the newer version of the code to these CMOD simulations.

Finally we note that all simulations discussed in this memo assume significant pumping by the plasma facing surfaces. Such pumping is not expected for an all metal device such as CMOD. However we seek fully steady state solutions so we would require a density profile which has zero gradient on the inner most surface (no ion current across this surface) , and no externally introduced neutrals.

That is we can not allow any particle input to the calculation domain if we eliminate all pumping. This does not seem consistent with the experiment, so we have introduced the wall pumping. This issue should be examined in more detail in future simulations.

5 Acknowledgement

This work performed under the auspices of the U.S. Department of Energy by Lawrence Livermore National Laboratory under Contract DE-AC52-07NA27344.

6 References

[1] T. Rognlien, J. Milovich, M. Rensink, and G. Porter, J. Nucl. Mater. 196-198 (1992) 347.

[2] B. LaBombard, J. L. Terry, J. W. Hughes, D. Brunner, J. Payne, M. L. Reinke, Y. Lin, and S. Wukitch, J. Nucl. Mat. submitted (2010)

[3] L. L. Lao, H. S. John, R. D. Stambaugh, A. G. Kellman, and W. Pfieffer, Nucl. Fusion 25 (1985) 1611.

[4] T. D. Rognlien, G. D. Porter, and D. D. Ryutov, J. Nucl. Mat. 266-269 (1999) 654.

[5] F. Wising, D. A. Knoll, S. I. Krasheninnikov, T. D. Rognlien, and D. J. Sigmar, Contrib. Plasma Phys. 35 (1996) 136.

[6] G. D. Porter, J. A. Boedo, T. N. Carlstrom, R. J. Groebner, M. J. Schaffer, P. C. Stangeby, T. D. Rognlien, M. E. Rensink, and N. S. Wolf, in 28th European Physics Society Conference on Controlled Fusion and Plasma Physics, Madeira, Portugal, 2001.